Ultrasound-Assisted Extraction of Polysaccharides from *Pleurotus ostreatus* By-Products: Box–Behnken Optimization and Low-Fat Cookies Formulation

P. Bermúdez-Gómez *, V. Grifoll, P. Bravo, M. Pérez-Clavijo

Posted Date: 27 April 2026

doi: 10.20944/preprints202604.1790.v1

Keywords: mushrooms by-products; *Pleurotus ostreatus*; Box-Behnken design; total dietary fiber; low-fat cookies; starch digestibility; glycemic index

 doi:10.20944/preprints202604.1790.v1

Article

Ultrasound-Assisted Extraction of Polysaccharides from *Pleurotus ostreatus* By-Products: Box–Behnken Optimization and Low-Fat Cookies Formulation

P. Bermúdez-Gómez *, V. Grifoll, P. Bravo and M. Pérez-Clavijo

Mushroom Technological Research Center of La Rioja (CTICH), Carretera Calahorra, KM 4, 26560 Autol, La Rioja, Spain

* Correspondence: patricia.bermudez@goumh.umh.es

Abstract

Spent mushroom substrate (SMS), the main by-product of mushroom production, is rich in valuable compounds that could be recovered by ultrasound-assisted extraction (UAE) and exploited as fat-mimetic functional ingredients in food formulations. In this study, low-fat cookies prototypes were developed by incorporating a dietary fiber extract obtained from SMS using UAE. The extraction process was optimized following a Box–Behnken experimental design, identifying optimal conditions at a specific energy input of 200 J/mL, a particle size of 2 mm, and a solute-to-solvent ratio of 1:27, yielding a dietary fiber recovery of 30.82%. The optimized SMS extract exhibited high oil-holding capacity (1.39 g/g), emulsion stability (80%), and foaming capacity (83.55%). Four cookie formulations were evaluated, among which G1 (50% fat replacement) showed the best balance between consumer acceptability and an improved nutritional profile, characterized by higher protein (8.4 g/100 g), total dietary fiber (7.10 g/100 g), and mineral contents. Notably, G1 cookies displayed a significant reduction in predicted glycemic index, decreasing from 83.84 in the control to 69.65. Overall, these results demonstrate that optimized SMS-derived dietary fiber is an effective functional ingredient for the development of low-fat, high-fiber, and reduced-glycemic cookies, contributing to the valorization of agro-industrial by-products within a circular economy framework.

Keywords: mushrooms by-products; *Pleurotus ostreatus*; Box-Behnken design; total dietary fiber; low-fat cookies; starch digestibility; glycemic index

1. Introduction

The global edible mushroom market has expanded significantly in the last years, with production expected to exceed 20 million tons annually by 2026 [1,2]. Among the most widely cultivated species is the oyster mushroom (*Pleurotus ostreatus*), an edible mushroom that grows on lignocellulosic materials originating from forest sources as well as from agricultural and food industry by-products [3]. During the commercialization of fruiting bodies, considerable quantities of by-products are produced, mainly consisting of spent mushroom substrate (SMS), stems, and mushrooms without the required size or shape for commercial sale outs [2]. Spent mushroom substrate consists of fungal mycelia, nutrients, extracellular enzymes secreted by mushrooms, and a wide range of disintegrated lignocellulosic biomass, such as sawdust, corn cob, straw, and wood chips [4,5]. Consequently, SMS contains a range of valuable compounds, including trace elements (Fe, Ca, Zn, and Mg), cellulose, hemicellulose, lignin, and crude protein [5]. Approximately 5 kg of SMS is released for every 1 kg of fresh mushrooms produced, resulting in the generation of about 60 million tons of this by-product annually, posing a significant challenge for producers [2,6,7]. Traditionally, mushroom by-products are disposed of by spreading them on farmland or subjecting them to incineration, open burning, landfilling, or composting with animal waste [4,8]. These practices result in environmental impacts, such as soil and water contamination [1,6]. Moreover, they

 doi:10.20944/preprints202604.1790.v1

lead to the loss of significant quantities of organic matter with high nutritional value, representing both an economic and ecological concern [1,5,6,9].

Hot water extraction followed by precipitation with alcohol is an extended technique used for water-soluble polysaccharide extraction [10]. However, these methods require long extraction times and high temperatures [11]. To mitigate these issues, green and novel extraction technologies, including ultrasound-assisted extraction (UAE), have emerged as an alternative for the recovery of bioactive compounds [12]. The improvement in extraction efficiency associated with ultrasound application is primarily attributed to acoustic cavitation phenomena generated in the solvent by ultrasonic waves [13]. These effects promote the disruption of cell wall structures and enhance mass transfer by accelerating diffusion across cellular membranes [13,14]. UAE has proven to be highly effective for the valorization of agro-industrial by-products through the isolation of a wide range of bioactive compounds, as it significantly reduces extraction time and solvent consumption [12,15]. The UAE has been investigated for the extraction of phenolic compounds and polysaccharides from spent mushroom substrate (SMS) derived from various edible mushroom species [12,16–18]. The extraction of polysaccharides from *Pleurotus ostreatus* SMS has been studied using an experimental design 2^3 that explored the effect of temperature and sonication time on extraction efficiency [17].

Fats and oils play a crucial role in cookie quality, affecting both mechanical and sensory properties [19]. Fat enhances dough spread during baking, reduces fracture stress, increases cookie tenderness, and improves flavor and aroma [19,20]. However, the rising consumer interest in healthy diets and the link between high lipid intake and metabolic disorders have prompted the food industry to develop reduced-fat products and explore fat replacers [20,21]. Fat replacers can be carbohydrates or proteins that could imitate the functional and sensory properties of fat [20–22]. Proteins such as lupin and carbohydrates such as inulin or hydroxypropyl methylcellulose have been extensively studied and have demonstrated good properties and positive results in sensory analysis by reducing the fat content of cookies [20–23]. These compounds not only enable fat reduction but also provide health benefits, as dietary fiber is associated with improved gastrointestinal function and a reduced risk of metabolic and cardiovascular diseases [22–24]. The use of spent mushroom substrate (SMS) as a food ingredient has so far been mainly investigated as a wheat flour substitute in bread [3]. However, its high dietary fiber content makes SMS a promising candidate for fat and flour replacement [3,17]. In addition, several studies have reported that polysaccharides derived from SMS exhibit relevant bioactivities, including antibacterial, antitumor, antioxidant, and renoprotective effects [25–28].

To expand the current understanding of UAE, this study investigates the impact of specific energy input, particle size, and solute-to-solvent ratio on the recovery of polysaccharides from *P. ostreatus* SMS. A Box-Behnken Design (BBD) was employed to optimize the extraction process. Subsequently, the functional role of the extract was tested as a fat and flour substitute in cookies, evaluating their physicochemical properties, sensory profile, and *in vitro* digestion kinetics to promote the integration of mushroom by-products into the circular food economy.

2. Methodology

2.1. Sample Preparation

The spent mushroom substrate (SMS) (wheat straw, corn husk, and urea) was defined as the residual matrix remaining after harvesting the fruiting bodies of *Pleurotus ostreatus* following two production flushes [26]. Cultivation was carried out at the CTICH facilities using the Alerpo strain, with spawn purchased from Amycel. Fresh SMS was dried in a dehydrator at 50 °C until a constant weight was reached (69.66% CH, 59.23% TDF: 26.80% celulosa, 15.41% hemicelulosa, 7.93% lignina, 17% Ash, 6.90% proteins). The dried mushroom by-product was then milled using an ultracentrifugal mill (ZM 200, Retsch™, Düsseldorf, Germany) equipped with four interchangeable sieves to obtain powders with particle sizes of 4 mm, 2 mm, 1 mm, and 0.25 mm. All powders were vacuum-packed and stored at room temperature in the dark.

 doi:10.20944/preprints202604.1790.v1

2.2. Ultrasound-Assisted Extraction of Water-Soluble Polysaccharides (WSP)

The ultrasound-assisted extraction of water-soluble polysaccharides (WSP) from dried *Pleurotus ostreatus* spent mushroom substrate (SMS) powders was performed using an ultrasonic generator (UIP2000hdT, Hielscher Ultrasonics GmbH, Schwabach, Germany) with thermostatic temperature control. SMS powders were mixed with distilled water and subjected to ultrasound treatment under varying conditions of specific energy input, solute-to-solvent ratio, and particle size. The extraction temperature was continuously monitored and maintained between 70 and 80 °C throughout the process. After sonication, the suspensions were filtered to remove solid residues, and the resulting filtrates were concentrated using a rotary evaporator (R-220 PRO, Büchi, Flawil, Switzerland). The concentrated extracts were then mixed with absolute ethanol (≥99.8%, PanReac AppliChem, Barcelona, Spain) at a 1:4 (v/v) ratio and allowed to stand for 16 h at room temperature to precipitate polysaccharides. The precipitates were collected by filtration, freeze-dried (Alpha 1–2 LD plus, Christ, Sigma Laborzentrifugen GmbH, Osterode am Harz, Germany), and milled. The percentage of polysaccharides yield (%) was also calculated following Equation (1).

$$\text{Yield } (\%\, w/w) = \frac{\text{Weight of dried crude extraction}}{\text{Weight of SMS powder}} \times 100 \quad (1)$$

2.3. Single-Factor Experiment Design

In this experiment, the following three variables were investigated: specific energy input (J/mL), particle size (mm), and solute-to-solvent ratio (%). Their variable effects on the WSP extraction yield were assessed. Each sample was extracted according to the above-mentioned procedure for polysaccharide extraction.

2.4. Optimization of Ultrasound-Assisted Extraction

The optimal conditions for ultrasound-assisted extraction were determined by response surface methodology (RSM) using a Box-Behnken Design (BBD). Through the single-factor experiment, the appropriate ranges of the independent variables: specific energy input (A), particle size (B), and solute-to-solvent ratio (C) were selected. Table 1 shows the range and center point values of the three independent variables. The BBD in experimental design consisted of 15 experimental runs, including 13 factorial points, and 3 replicates at the central point; each experiment was performed in triplicate. Experimental runs were randomized to minimize the effects of uncontrolled variability. The three variables at the three levels were coded as -1, 0, and +1.

Table 1. Levels and codes employed in the present study for the construction of Box-Behnken Design (BBD).

Variables	Codes	Levels		
		-1	0	+1
Specific energy input (J/mL)	A	200	350	500
Particle size (mm)	B	0.25	1.125	4
Solute-to-solvent ratio (%)	C	15	27.5	40

The yield (%) of WSP and the total dietary fiber content (%) were chosen as the response or dependent variables (Y). Total dietary fiber (TDF) was analyzed by a standardized enzymatic-gravimetric method Megazyme Total Dietary Fiber Kit (K-TDFR, Megazyme, Wicklow, Ireland), according to the AOAC Official Method 991.43 [29].

2.5. Proximate Composition

All determinations were performed in triplicate and expressed as g/100 g of dry weight. Proximate compositions were estimated using methods based on the Association of Official Analytical Chemists [30]. Moisture contents were calculated using the difference in weight after drying in an ED 400 stove (Binder GmbH, Tuttlingen, Germany) at 105 °C compared to the constant weight. Total ash was determined using a 10-PR/400 muffle (Hobersal, Barcelona, Spain) at 550 ◦C

 doi:10.20944/preprints202604.1790.v1

after 5 h crude protein was determined using the Kjeldahl method using a Kjeltec System 2200 nitrogen distiller (FOSS IBERIA, Barcelona, Spain) and a digestion block (FOSS IBERIA, Barcelona, Spain). Crude fats were extracted following the Folch method described by Eggers and Schwudke [31]The samples were briefly hydrolyzed with HCl (3 M) for 1 h at 80 ◦C in a LSB18 shaking bath (VWR International Eurolab, Barcelona, Spain), and finally, fat was extracted via dilution (1:20, v/v) with chloroform:methanol (2:1, v/v). Total carbohydrates were calculated by subtracting moisture, total fat, protein, and ash at 100%.

2.6. pH and Instrumental Color

The pH of the optimized WSP extract was measured by mixing 5 grams of the sample with 40 mL of ultrapure water. After 10 min of stirring, the pH was assessed in a pH meter GLP 21 (Crison Instrument S.A., Barcelona, Spain). The color was measured with a chroma meter CR-400 colorimeter (Konica Minolta, ITA Aquateknica S.A., Valencia, Spain) with illuminant D65, observer 2°, SCI mode, 8 mm aperture for illumination and measurement, based on the CIELab color space. The following color coordinates were determined: lightness (L*), redness (a* ± red-green), and yellowness (b* ± yellow-blue).

2.7. Techno-Functional Properties

Water holding capacity was determined by adding 10 mL of ultrapure water to 500 mg of the extract. Subsequently, the mix was stored at room temperature for 18 h. After being centrifuged (4780 rpm, 20 min), the supernatant was discarded, and the pellet was weighed [32]. The WHC of each sample was expressed as the weight of water held per gram of the corresponding sample (g of water/g sample). Oil holding capacity (OHC) was determined following the same procedure, replacing water with oil. The results were expressed as grams of oil retained per gram of sample (g oil/g sample). Beuchat's method was employed for the determination of water absorption capacity (WAC). Briefly, 1 g of extract was mixed with 10 mL of distilled water and agitated for 1 h. The mixture was then centrifuged at 4750 rpm for 30 min, the supernatant was discarded, and the pellet was weighed. The results were reported as g of water held by g of sample (g/g) [33].

For the emulsifying capacity (EC), 1 g of extract was mixed with 50 mL of distilled water and agitated for 30 min. Subsequently, 50 mL of sunflower oil was added, and the mixture was agitated for an additional 30 min to form the emulsion. Then, 10 mL of the emulsion was transferred to graduated centrifuge tubes and centrifuged at 3000 rpm for 5 min to allow phase separation. The volume of the emulsified layer was measured and used to calculate the emulsifying activity of the extract as the percentage of the emulsified layer relative to the total volume in the centrifuge tube [34]. Emulsion stability (ES) was evaluated using the emulsions prepared for the emulsifying activity assay. The centrifuge tubes containing the emulsions were heated at 80 °C for 30 min, cooled to room temperature, and then centrifuged at 3000 rpm for 5 min. Emulsion stability was expressed as the percentage of the emulsified layer remaining relative to the initial emulsion volume.

Foaming capacity (FC) of the extract was determined following the method described by Coffmann and Garcia (2007) [35] Briefly, 1 g of extract was mixed vigorously with 50 mL of distilled water for approximately 5 minutes to generate foam using a stirring beaker. The resulting foam was carefully transferred to a graduated cylinder, and its initial volume was recorded. Subsequently, the foam volume was measured after 30 seconds to assess its stability. These values were used to calculate the foaming capacity and foam stability of the extract.

2.8. Cookie Development

Cookies were developed by utilizing various commercially available raw ingredients: wheat flour (125 g), butter (62.5 g), sugar (40 g), vanillin (20 g), egg white (16.25 g), cocoa (14.25 g), yeast (5 g), baking powder (1.25 g) and salt (0.125 g) (Table 2). This recipe was used as the control. The WSP extract was incorporated to partially replace butter at 50% (G1) and 75% (G3) In addition, two

 doi:10.20944/preprints202604.1790.v1

formulations combined the replacement of butter (50% or 75%) with a 10% substitution of wheat flour, corresponding to G2 and G4, respectively (Figure 1).

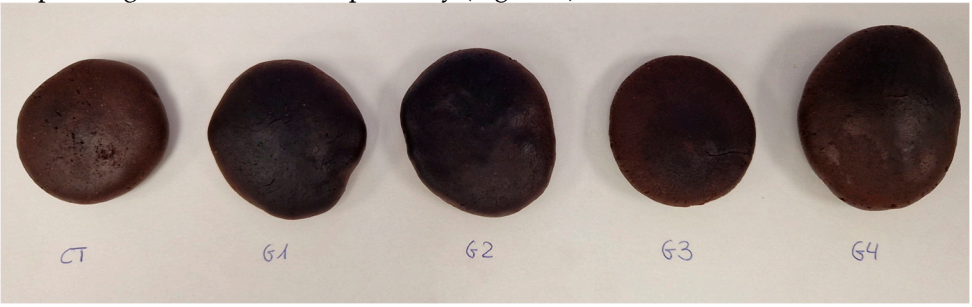

Figure 1. Low-fat cookies by the addition of SMS dietary fiber extract.

Cookie dough was prepared using an HM300 kneader (Kenwood Ltd., Havant, UK). Initially, sugar and eggs were creamed until homogeneous, followed by the incorporation of butter and, where applicable, the SMS extract. After achieving a creamy texture, cocoa powder, vanillin, and water were added. The remaining dry ingredients were then incorporated, and the mixture was kneaded for 5 min to ensure a consistent dough. The resulting dough was sheeted to a 5 mm thickness and molded into round pieces (3 cm diameter; 16 g weight). The samples were stored at –18 °C for a maximum of 10 days. Finally, the cookies were baked directly from frozen in an HR-38N RM7 electric oven (Grunkel, Madrid, Spain) at 200 °C for 12 min.

Table 2. Formulation of control cookies and low-fat prototypes by the addition of SMS extract.

Ingredients (g/250g)	CT	G1	G2	G3	G4
Wheat flour	125	125	112.5	125	112.5
Butter	62.5	31.25	31.25	15.6	15.6
Sugar	40	40	40	40	40
Extract	--	31.25	43.75	46.9	59.4
Vanilla	20	20	20	20	20
Egg	16.25	16.25	16.25	16.25	16.25
Cocoa	14.25	14.25	14.25	14.25	14.25
Water	-	7.5	10	15	25
Yeast	5	5	5	5	5
Baking soda	1.25	1.25	1.25	1.25	1.25
Salt	0.125	0.125	0.125	0.125	0.125

2.9. Chemical and Physicochemical Characterization

For the nutritional analysis of the biscuits, the contents of protein, fat, moisture, ash, and fiber were determined following the procedures described in Section 2.4. and Section 2.5. Instrumental color was assessed as outlined in Section 2.6. All analyses were conducted in triplicate.

2.10. Sensorial Analysis

Biscuits control and prototypes were submitted to a panel of 85 people (aged between 19 and 65 years old). Untrained consumers were recruited among staff at the Mushroom Technological Research Center of La Rioja (CTICH) and among local inhabitants. The sensory evaluation was conducted using cookie samples 1 hour after baking. Coded samples of biscuits (1 × 1 × 1 cm) with a random 3-digit number were given to the evaluation panel on white plates. Water was used to rinse the mouth before and after each sample test. The panelists were asked to score the following attributes on a nine-point hedonic scale, where 1 = dislike extremely, 5 = neither like nor dislike, 9 = like extremely: appearance, color, aroma, graininess, hardness, stickiness, sweet taste, bitter taste, and overall acceptability.

 doi:10.20944/preprints202604.1790.v1

2.11. In Vitro Digestion: Starch and Predicted Glycemic Index

In vitro gastrointestinal digestion was done following the harmonized INFOGEST protocol (V 2.0) [36]. Prior to initiating the digestion process, the cookie samples were ground and passed through a 510 µm mesh sieve to simulate the particle size typically resulting from mastication. In brief, 500 mg of milled biscuits was mixed with 500µL of distilled water to obtain a pasta with tomato pasta consistency. Then, simulated salivary fluid with salivary alpha-amylase (75 U/mL) (α-Amylase from human saliva, Type XIII-A, 940 U/mg protein) was added, followed by incubation in agitation at 37ºC and 60 rpm. After 2 minutes, 1.6 mL of simulated gastric fluid and HCl (1 M, 0.25M) until pH 3.0 was incorporated into the oral samples to stop oral digestion. After that, 100µL of porcine pepsin solution (2000 U/mL) (Sigma-Aldrich P7012) was added. Then the samples were incubated in the same conditions as the oral phase for 2 h. Finally, the gastric phase was mixed with 1.7 mL of simulated intestinal fluid, 8µL of CaCl2 (3M), 0.5 mL of bile (Bile bovine B3883-25G), and 1 mL of pancreatin (Sigma Pancreatin P7545 8 x USP specifications). The pH was adjusted to 7.0 with NaOH (1M, 0.25M), and the samples were incubated for 2 h at 37ºC and 60 rpm of agitation. Starch hydrolysis after *in vitro* gastrointestinal digestion was monitored in the oral phase (2 min), at the two points of the gastric phase (20 and 120 min), and at three points of the intestinal phase incubation (140, 210, and 240 min). A heat shock (100ºC, 5 min) was carried out to inactivate digestive enzymes in the gastric and intestinal phases, and a pH shift to 3 was carried out to inactivate digestive enzymes in the oral phase. For the respective five points studied, an individual *in vitro* digestion was performed. The simulated digestion of 6 different endpoints was achieved in triplicate for all the cookies. After the digestive enzymes were inactivated, the digested samples were centrifuged at 10,000 rpm for 10 min.

Regarding the starch, two aliquots of 0.45 mL were taken from each studied digestive endpoint and mixed with sodium acetate (100 mM) plus ClCa2 (5 mM), pH 5.0 (Dilution 1:4), and amyloglucosidase (20 µL; 60 U/mL) to complete the digestion of glucose disaccharides and oligosaccharides. The samples were incubated at 50ºC for 30 min. After that, the samples were diluted (1:10). Finally, aliquots of 50µL digestive dilution were mixed with GOPOD reactive (1.5 mL) and incubated for 30 min at 50ºC. Then the absorbance of the samples was measured at 510 nm. Blank was carried out by substituting samples with sodium acetate (100 mM) plus ClCa2 (5 mM), pH 5.0. Three glucose patterns (1 mg/mL) were included in each reaction. To avoid over-starch hydrolysis estimation after *in vitro* gastrointestinal digestion, a blank with a sample but without enzymes was used for each batch. Equation (2) was used to calculate the percentage of starch after *in vitro* digestion.

$$\%\text{Starch} = \Delta A \times F \times \frac{VD}{0.05} \times D \times \frac{1}{1000} \times \frac{100}{W} \times \frac{162}{180} \quad (2)$$

Where,

A = Absorbance sample

F = factor to convert absorbance values to µg of D-glucose (100 µg of D-glucose divided by the GOPOD absorbance value for 100 µg of D-glucose)

VD = Digestion phase volume (mL)

D = Dilution factor

W = Sample dry weight (mg)

162/180 = Factor to convert from free glucose, as determined, to anhydroglucose, as occurs in starch.

Finally, to assess the percentage of hydrolyzed starch content, total starch content was determined using the AOAC Official Method 996.11 with a previous alcohol washing with the help of a total starch kit (Megazyme, Bray, Ireland). Predicted glycemic index (pGI) was calculated as the area under the curve (AUC) of each studied bread formulation, with the help of the first-order equation of the hydrolytic process (Equations (3) and (4), using white bread as reference food. Equations (5)and (6) proposed by Goñi et al. were also used for calculating the pGI [37]. The concentrations obtained at 210 min were used as the final reaction time.

$$C = C_\infty (1 - e^{-kt}) \quad (3)$$

$$AUC = C_\infty (t_\infty - t0) - (C_\infty / k)\left[1 - e^{-k(t_\infty - t0)}\right] \quad (4)$$

 doi:10.20944/preprints202604.1790.v1

$$I = AUC_{cookie} / AUC_{white\ bread} \times 100 \quad (5)$$

$$pGI = 39.71 + 0.549\ HI \quad (6)$$

Where,
C = % hydrolyzed starch
C_∞ = % hydrolyzed starch at final time
k = kinetic reaction constant
t_∞ = final reaction time (140 min)
t_0 = start reaction time

2.12. Statistical Analysis

All the results are presented as the mean ± standard error of the mean (SEM) of at least three independent, triplicate measurements. Data obtained for all the determinations were analyzed using one-way ANOVAs. Tukey's post hoc test was applied for comparisons of means; differences were considered significant at $p < 0.05$. The extraction of total dietary fiber was optimized using a Box–Behnken design. Experimental data were fitted to a second-order polynomial model using Statgraphics (Centurion 19-X64). The fitting quality of the model was evaluated by Analysis of Variance (ANOVA), specifically considering the coefficient of determination (R^2). Finally, the predicted values and regression equations obtained from Statgraphics were used to construct the response surface plots in OriginPro 2026 (OriginLab Corporation, Northampton, MA, USA) for enhanced graphical visualization as well as the radial plot for sensorial evaluation. The applied polynomial model was Equation (7):

$$Y = \beta_0 + \sum_{i=1}^{k} \beta_i X_i + \sum_{i=1}^{k} \beta_{ii} X_i^2 + \sum_{i<j}^{k} \beta_{ij} X_i X_j + \varepsilon \quad (7)$$

where Y is the dependent variable, β0 is the independent term, βi are the linear regression coefficients, βii are the quadratic regression coefficients, βij are the interaction regression coefficients, Xi or Xj and the independent variables or factors, and k is the number of independent variables or factors. To compare the experimental vs. theoretical values, a validation analysis was performed at a 95% confidence level, where a p-value greater than 0.05 means no significant statistical difference.

3. Results and Discussion

3.1. Optimization of Ultrasound-Assisted Extraction

The Box–Behnken design was applied to evaluate and optimize the extraction of total dietary fiber from SMS powder as a function of three independent variables (specific energy input, particle size, and solute-to-solvent ratio), with a recognized effect on UAE efficiency [14,38]. The parameters considered during UAE fiber optimization were specific energy input (200 – 500 J/mL), particle size (0.25 – 2 mm), and solute-to-solvent ratio (15 – 40 %). This range of studied variables was selected based on results from preliminary experiments (Figure S1) and previous studies on UAE for the extraction of polysaccharides from SMS in edible mushrooms [16,18]. Based on these results, a higher specific energy input (400 J/ml) increased extraction yield (19.21%) compared to 100 J/mL (17.53%) ($p < 0.05$), in agreement with previous reports [11,38]. At a constant volume and amplitude, as applied in this study, specific energy is directly related to sonication time. From 100 W to 400 W, fiber yield increased rapidly; however, a maximum yield was reached at 400 W, beyond which no further improvement was observed. A similar trend has been previously reported for sonication time [39]. Regarding particle size, a higher extraction yield was observed as particle size decreased from 1 mm (18.72 %) to 0.25 mm (21.85 %). This behavior can be attributed to the increased surface area available for solvent contact, which enhances mass transfer [40].

 doi:10.20944/preprints202604.1790.v1

Table 3. Experimental matrix of the Box–Behnken design for the extraction of polysaccharides from SMS powder. The values correspond to the average of three independent trials ± standard e rror of the mean (SEM).

Experiments	A	B	C	TDF (%)
1	200	0.25	27.5	29.87^{d}±0.25
2	200	2.00	27.5	39.71^{a}±0.65
3	500	0.25	27.5	33.84^{c}±0.35
4	500	2.00	27.5	38.28^{ab}±0.20
5	350	0.25	15	40.90^{a}±0.53
6	350	2.00	15	38.26^{ab}±0.59
7	350	0.25	40	29.95^{d}±1.18
8	350	2.00	40	36.42^{bc}±0.14
9	200	1.00	15	31.67^{cd}±0.65
10	500	1.00	15	32.23^{cd}±0.11
11	200	1.00	40	31.60^{cd}±0.33
12	500	1.00	40	23.27^{e}±0.19
13	350	1.00	27.5	31.10^{cd}±0.70
14	350	1.00	27.5	31.51^{cd}±1.07
15	350	1.00	27.5	30.72^{d}±0.35

A: specific energy input, B: Particle size, C: solute-to-solvent ratio, TDF: total dietary fiber.

Finally, to assess both the individual effects and the interactions among the independent variables on the response, a second-order polynomial equation (quadratic model) was used. The experimental matrix and the corresponding TDF content are presented in Table 3. A total of 15 experimental runs were carried out, including three replicates at the center point to estimate the experimental error and assess the model reproducibility. The TDF content varied significantly across the experimental domain ($p < 0.05$), ranging from 23.27% to 40.90%, indicating a strong dependence of the extraction efficiency on the selected process variables (Table 3). The highest TDF value ($p < 0.05$) was obtained at intermediate levels of specific energy input combined with the lowest level of particle size and the lowest level of solute-to-solvent (experiment 5). In contrast, the lowest TDF amount ($p < 0.05$) was observed at high levels of specific energy input and solute-to-solvent ratio with an intermediate level of particle size (experiment 12). These results suggest the presence of significant interactions among the studied factors, which were further confirmed by the fitted response surface model.

By applying multiple regression analysis on the experimental data, the response and test variables were found to correlate by the following second-order polynomial equation (*8*):

$$Y = 28{,}3858 + 0{,}0742623\times A - 15{,}4129\times B + 0{,}0469339\times C - 0{,}0000516654\times A2 - 0{,}00884597\times A\times B - 0{,}00119018\times A\times C + 7{,}0195\times B2 + 0{,}193959\times B\times C - 0{,}000965527\times C2 \quad (8)$$

where Y is the Total Dietary Fiber, and A, B and C are the coded variables specific energy input, particle size and solute-to-solvent ratio, respectively.

Table 4 summarizes the results of the analysis of variance, goodness-of-fit, and the adequacy of the model. The model's reliability was established using the Durbin-Watson (DW) statistic and a comparative analysis of the determination coefficients (R^2). The R-value for Eq. (*8*) was 0.8584, which was relatively high, indicating a close agreement between experimental and predicted values of the TDF amount. The R^2 adjusted is the correlation measure for testing the goodness-of-fit of the regression equation. The value R^2 adjusted for Eq. (*8*) was 0.8307, which indicates that 83.07% of the total variation in the content was attributed to the experimental variables studied. Furthermore, the R^2 predicted for Eq. (*8*) was 0.7862. The obtained DW value of 2.374 (p = 0.9010) confirms the absence of significant serial autocorrelation in the experimental data ($p > 0.05$). This result ensures that the variations in TDF content are due to the factors studied and not to systematic experimental errors, providing high reliability to the ANOVA results. The precision of the mathematical fit was further

 doi:10.20944/preprints202604.1790.v1

evidenced by the standard error of the estimate (1.9314) and the mean absolute error (MAE = 1.4912). These values, expressed in the same units as the response variable (%), indicate a high level of accuracy in the model's predictions. The low MAE value suggests that the average deviation between the experimental and predicted total dietary fiber content is minimal, confirming the reliability of the Box-Behnken design for this extraction process.

Table 4. Statistical parameters for the fitted model validation.

Statistic	Value
R-squared (R^2)	85.84%
Adjusted R-squared	83.07%
Predicted R-squared	78.62%
Durbin-Watson statistic (*p*-value)	2.37 (0.9010)
Standard Error of the Estimate	1.9314
Mean Absolute Error (MAE)	1.4912

The adequacy of the model was further justified through analysis of variance (ANOVA), Table 5. The significance of each coefficient was evaluated using the P-value. Variables are considered more significant when the F-value is higher, and the P-value is lower. Additionally, the P-value can be used to assess the strength of interactions between independent variables [10]. In this case, the independent variables (B and C), the interaction terms (AA, AB, AC, BB, and BC) significantly affected the content of TDF. Ultrasonic energy alone did not exert a significant main effect but showed negative interactions with the solute-to-solvent ratio (AC). High specific energy input, combined with an elevated solvent ratio, decreased TDF extraction by reducing the effect of cavitation intensity in the SMS powder [38]. Particle size exerted a dominant positive effect, particularly in its quadratic form (BB, $p < 0.0001$). These results differ from established mechanisms where reduced particle size enhances specific surface area, allowing ultrasonic cavitation to accelerate cell wall disruption [41]. However, excessive grinding may increase viscosity, limiting cavitation intensity and hindering fiber solubilization [42]. Finally, the interaction between particle size and ratio was significantly positive ($p = 0.0001$), reinforcing the synergy between solvent availability and high specific surface area for enhanced mass transfer, aligning with previous reports of UAE extraction of dietary fiber [43].

Table 5. Analysis of Variance (ANOVA) for the quadratic model of Total Dietary Fiber (TDF) extraction from SMS *Pleurotus ostreatus*.

Variables	Estimated Effect (pred)	Standard Error	Estimated effect (adj)	Sum of square	Df	Mean Sum of Squares	F-value	P-value
A: Specific energy input	-1.3755	0.8871	0.0432	14.4453	1	14.4453	3.87	0.0551
B: Particle size	4.5829	0.8833	-18.4114	161.728	1	161.728	43.36	0.0000*
C: LSR	-5.1132	0.9098	-0.3049	189.739	1	189.739	50.87	0.0000*
AA	-0.3259	1.3354	-0.000007	18.2239	1	18.2239	4.89	0.0321*
AB	-2.3221	1.2195	-0.0088	21.7796	1	21.7796	5.84	0.0197*
AC	-4.4632	1.2719	-0.0012	73.9783	1	73.9783	19.83	0.0001*
BB	12.7893	1.3663	8.3522	371.749	1	371.749	99.66	0.0000*
BC	4.2429	1.2721	0.1940	66.8316	1	66.8316	17.92	0.0001*
CC	1.6973	1.3369	0.0054	0.3080	1	0.3080	0.08	0.7758
Total Error				171.588	46	3.7302		
Total (corr.)				1211.90	55			

*Stadistically significance (p<0.05). LSR: Solute-to-solvent ratio, Df: Degree of freedom, SE: Standard error.

Based on the data obtained from Eq. (*8*) using RSM, three-dimensional response surface plots were generated to visualize the relationships between the responses and the processing variables, as

 doi:10.20944/preprints202604.1790.v1

well as the interactions between pairs of variables. These plots were constructed by representing the TDF content on the *Z*-axis as a function of the two processing variables that showed significant effects.

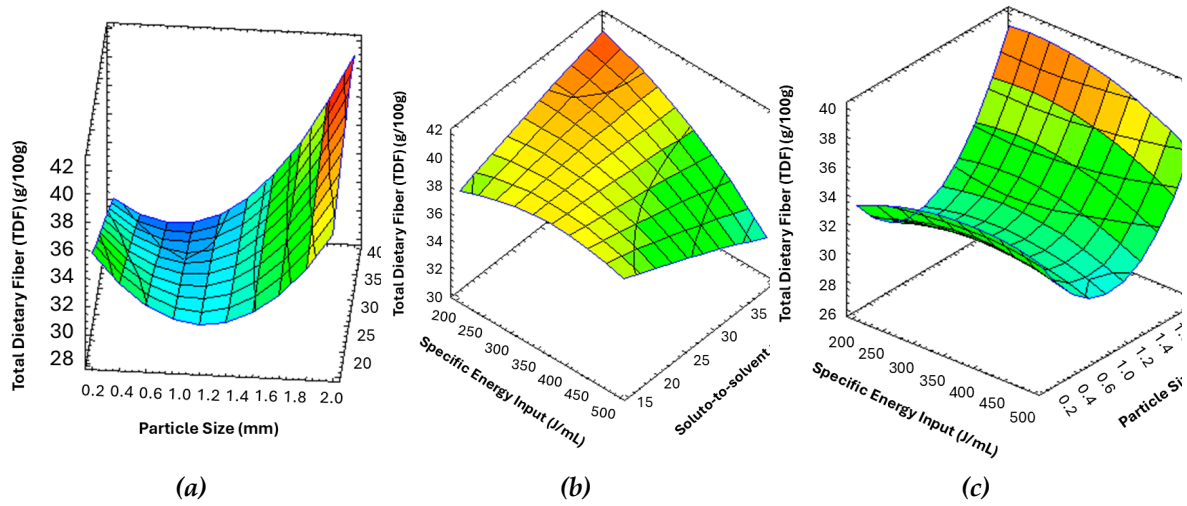

Figure 2. Response Surface plots showing the interactions between process parameters (a) Solute-to-solvent ratio and Particle size, (b) Solute-to-solvent ratio and Specific energy input and (c) Particle size and Specific energy input.

Figure 2a illustrates the three-dimensional response surface plot describing the combined effect of solute-to-solvent ratio and particle size on total dietary fiber (TDF) content. An overall increasing trend in TDF was observed with increasing particle size, particularly at higher solute-to-solvent ratios. At low particle sizes, TDF values remained comparatively low regardless of the solute-to-solvent ratio; however, as particle size increased, a marked enhancement in TDF content was evident. The highest TDF values were obtained at the upper levels of both variables, indicating a significant interaction between particle size and solute-to-solvent ratio on TDF yield. Figure 2b shows the three-dimensional response surface plot at varying solute-to-solvent and specific energy input. It could be seen that the maximum extraction of polysaccharides could be achieved when the specific energy input was lower, and the solute-to-solvent ratio was higher. Figure 2c shows the three-dimensional response surface plot at varying specific energy input and particle size. It could be seen that the maximum extraction of polysaccharides could be achieved when the specific energy input was lower, and the particle size was larger.

The optimal extraction conditions obtained in the present study were specific energy input 200 J/mL, particle size 2 mm, and solute-to-solvent ratio 1:27. Under these conditions, the response value predicted by the model was 39.60%

3.2. Characterization of Optimized Dietary Fiber Extracts

The extraction conditions were validated by means of five independent extractions. The results of the characterization of this optimized extract in terms of chemical composition, physicochemical characteristics, and techno-functional properties are shown below.

3.2.1. Proximate Composition of Dietary Fiber Extract

The proximate composition of the optimized SMS extract is presented in Table 6. The extraction process significantly modified the chemical profile of the substrate. Specifically, the protein content increased from 6.9 g/100 g of dehydrated SMS to 14 g/100 g in the SMS extract. This behavior contrasts with previous reports on ultrasound-assisted extraction of polysaccharides from SMS, where a decrease in protein content after extraction was observed [16]. This discrepancy may be attributed to differences in ultrasound application, as that study employed an ultrasonic bath, which provides lower ultrasonic power compared to a probe system [38]. Consequently, the higher ultrasonic intensity applied in the present study may have promoted the solubilization of a greater amount of

 doi:10.20944/preprints202604.1790.v1

protein, since ultrasound-assisted extraction is inherently non-selective [38]. In addition, proteins could precipitate in the presence of ethanol [44]. Other studies have highlighted differences between purified and non-purified SMS polysaccharide extracts obtained through protein removal using the Sevag method [45]. These studies reported not only a reduction in protein content but also a reduced antioxidant activity and phenolic compounds [45]. Considering these findings, together with the potential health and technological beneficial effects of protein–polysaccharide complexes, extract purification was intentionally avoided in the present study [45–47].

Regarding total dietary fiber, a significant reduction was observed in the optimized extract (30.82 g/100 g) compared to dehydrated SMS (59.23 g/100 g) ($p < 0.05$). It should be noted that the extraction process leads to the loss of insoluble dietary fiber, as the fraction not dissolved in the solvent is discarded during extraction. Consequently, the water-soluble polysaccharides recovered from SMS are mainly composed of soluble dietary fiber, particularly hemicelluloses [4,6,48]. In dehydrated SMS, the hemicellulose content accounted for 15.41%, supporting this hypothesis. In addition, ultrasound-assisted extraction may promote partial cellulose degradation into shorter chains, thereby increasing their solubility [41]. About total carbohydrates, a decrease was also observed, from 69.66% in the dehydrated SMS to 55.4% in the extract, suggesting a partial removal of the non-structural carbohydrate matrix during optimization. Similar carbohydrate contents have been reported in polysaccharide extracts obtained from *Pleurotus* SMS [16,45]. Finally, a notable increase in ash content was observed in the SMS extract (23.0 g/100 g) compared to the dehydrated SMS (17.0 g/100 g), indicating a concentration of mineral compounds. According to Regulation (EU) No 1047/2012, the extract could be considered high in calcium, magnesium, iron, manganese, zinc, and copper [49].

Table 6. Proximate composition of optimized dietary fiber extract.

Sample	Protein	Fat	CH	TDF	Ash	Ca	Mg	Fe	Mn	Zn	Cu
SMS extract	14.0± 0.11	1.40± 0.06	55.4± 0.56	30.82± 0.52	23.0± 0.23	4211.8 ± 5.13	663.6± 0.01	66.10± 0.43	52.00± 0.68	20.30± 0.33	2.27± 0.02

Results are reported as mean ±SEM (n=3). Results of protein, fat, CH, TDF, and ash are expressed as g/100g of dried weight. Results of minerals are expressed as mg/100g of dried weight. CH: carbohydrates, TDF: total dietary fiber. Ca: calcium, Mg: magnesium, Fe: iron, Mn: manganese, Zn: zinc. Cu: copper.

3.2.2. Water Activity, pH, and Instrumental Color Parameters of Dietary Fiber Extract

The physicochemical parameters of the extract are observed in Table 7. The extract presented a pH of 5.60 ± 0.01 and a low water activity (a_w) of 0.11 ± 0.01, which ensures a low risk of deterioration caused by microbial activity and enzymatic or non-enzymatic reactions, and therefore a long shelf-life for the dehydrated ingredient. The SMS extract exhibited a lightness (L*) value (67.13) that was higher than that reported for some dietary fiber extracts, but lower than values described for others [50,51]. Regarding redness (a*) and yellowness (b*), values of 4.47 and 21.46, respectively, were higher than those reported for soluble dietary fiber extracted from other agro-industrial by-products [50,51]. These color characteristics may be associated with the co-extraction of pigments during ultrasound-assisted optimization [38,45]. Overall, these instrumental color parameters should be carefully considered when incorporating the extract into food formulations, as they may induce noticeable color changes in the final product [50].

Table 7. Physicochemical parameters of dietary fiber extract.

Sample	pH	a_w	L*	a*	b*
SMS extract	5.60± 0.01	0.11± 0.01	67.13± 0.33	4.47± 0.15	21.46± 0.43

Results are reported as mean ±SEM (n=3). a_w: water activity, L*: lightness, a*: redness, and b*: yellowness.

3.2.3. Techno-Functional Properties of Dietary Fiber

 doi:10.20944/preprints202604.1790.v1

The techno-functional properties of the optimized SMS extract are summarized in Table 8. Regarding hydration properties, the extract showed low WHC (0.24 g/g) and WAC (0.06 g/g). This could be due to SMS dietary fiber extract composition, which mainly consisted of soluble dietary fiber (SDF) or water-soluble polysaccharides with high solubility [43]. However, in this case, the extract did not fully solubilize in water, in contrast to what had been previously reported for other soluble fiber sources [43]. Although ultrasound application may enhance water interactions by promoting the exposure of hydrophilic groups, such as hydroxyl and carboxyl groups on the SDF surface, excessive ultrasound treatment can also induce drastic structural changes [41,42,52]. These changes may disrupt polysaccharide intermolecular interactions, leading to a less porous structure and, consequently, reduced water retention capacity [41,42,51,52]. A similar trend was observed for OHC, which was relatively low (1.39 g/g) but comparable to values reported for other dietary fiber-rich by-products, indicating potential applicability as fat mimetics [41,43,50,53]. OHC reflects the oil-binding ability of the SDF extract and is closely associated with fiber surface structure, hydrophobicity, and charge density [41]. In this context, the OHC observed for the extract may be partially attributed to the presence of proteins containing hydrophobic amino acids [41,52].

Regarding emulsifying properties, EC refers to the ability of a substance to reduce interfacial tension between immiscible liquids, whereas ES describes its ability to maintain the emulsion and its resistance to rupture [54,55]. The extract exhibited a low EC (5%), which is consistent with its WHC and OHC values. Nevertheless, polysaccharide–protein interactions could act as surfactants, reducing interfacial tension and stabilizing air-water or oil-water interfaces [54]. Accordingly, the extract showed high emulsion stability (80%). In addition, SMS polysaccharides may increase the viscosity of the aqueous phase and delay droplet coalescence, further contributing to emulsion stability [56]. This surface activity was also reflected in the high foaming capacity (83.55%) of the extract. Therefore, the optimized SMS extract shows promising stability of high-fat foods, such as cookies [51,56].

Table 8. Techno- functional properties of optimized dietary fiber extract.

Sample	WHC (g/g)	OHC (g/g)	WAC (g/g)	EC (%)	ES (%)	FC (%)
SMS extract	0.24± 0.08	1.39± 0.01	0.06± 0.00	5.00± 0.00	80.00± 0.00	83.55± 6.94

Results are reported as mean ±SEM (n=3). WHC: Water holding capacity, OHC: Oil holding capacity, WAC: Water absorption capacity, EC: Emulsifying capacity, ES: Emulsion stability, and FC: Foaming capacity.

3.3. Development and Characterization of Low-Fat Cookies by the Addition of Optimized Dietary Fiber Extract

After characterizing the composition as well as the physicochemical and techno-functional properties of the SMS extract, its application as a fat substitute in cookies was assessed. For this purpose, the nutritional profile, instrumental color, sensory properties, and digestibility were evaluated.

3.3.1. Nutritional Analysis of Low-Fat Cookies

The chemical composition of the control and the reformulated cookie prototypes is summarized in Table 9. Replacing butter and wheat flour with the optimized dietary fiber extract significantly altered the nutritional profile of the final products ($p < 0.05$). Specifically, formulations containing higher proportions of the extract (G3 and G4) showed increased moisture content compared to the control ($p < 0.05$), which may be attributed to the higher water addition required to facilitate dough handling in these formulations [57]. Regarding protein content, all reformulated cookies exhibited significantly higher values than the control ($p < 0.05$), with G4 showing the highest content (9.0 g/100 g) compared to 7.1 g/100 g in the control. This increase in protein content has not been commonly

 doi:10.20944/preprints202604.1790.v1

reported in cookies formulated with fat replacers based on complex carbohydrates [20,57]. However, similar enrichment in protein content has also been observed when wheat flour is partially replaced with polysaccharides derived from *Pleurotus* spp. [58]. As intended, a significant reduction in fat content was achieved in all formulations containing the SMS extract (6.1–10.0 g/100 g) compared to the control (18.0 g/100 g) ($p < 0.05$). The most pronounced reductions were observed in G3 and G4 (6.1 and 6.6 g/100 g, respectively), corresponding to a 75% butter replacement. Comparable fat contents to those of the control have been reported in previous studies using similar formulations [20,57,59]. Additionally, similar lipid reductions have been documented following the incorporation of inulin, polydextrose, and other complex carbohydrates [20,57,59].

Table 9. Nutritional composition and color of control and protypes of low-fat cookies by de addition of optimized dietary fiber extract. .

Parameters	Control	G1	G2	G3	G4
Moisture	$14.0^{c}\pm0.15$	$14.0^{c}\pm0.16$	$15.0^{b}\pm0.20$	$16.0^{a}\pm0.10$	$16.0^{a}\pm0.23$
Protein	$7.10^{c}\pm0.13$	$8.40^{b}\pm0.11$	$8.50^{ab}\pm0.10$	$8.80^{ab}\pm0.15$	$9.00^{a}\pm0.12$
Fat	$18.0^{a}\pm0.20$	$9.2^{b}\pm0.25$	$10.0^{b}\pm0.30$	$6.1^{c}\pm0.09$	$6.6^{c}\pm0.08$
Ash	$1.90^{e}\pm0.01$	$4.4^{d}\pm0.02$	$5.70^{c}\pm0.02$	$5.8^{b}\pm0.01$	$6.8^{a}\pm0.01$
CH	$55.7^{a}\pm0.30$	$56.90^{a}\pm0.35$	$52.50^{b}\pm0.25$	$56.20^{a}\pm0.30$	$53.70^{b}\pm0.27$
Energy (Kcal/100g)	$418.88^{a}\pm2.35$	$358.72^{b}\pm1.95$	$351.24^{b}\pm2.12$	$329.1^{c}\pm1.07$	$327.54^{c}\pm1.25$
TDF	$3.16^{d}\pm0.10$	$6.64^{c}\pm0.14$	$7.78^{b}\pm0.09$	$7.40^{b}\pm0.12$	$8.33^{a}\pm0.13$
Ca	$52.45^{e}\pm0.32$	$557.11^{d}\pm3.35$	$747.51^{c}\pm4.85$	$872.12^{b}\pm5.56$	$1000.0^{a}\pm6.69$
Mg	$48.26^{e}\pm0.25$	$130.5^{d}\pm1.25$	$161.55^{c}\pm1.35$	$170.76^{b}\pm1.15$	$199.84^{a}\pm1.89$
Fe	$2.72^{d}\pm0.06$	$7.94^{c}\pm0.12$	$9.69^{c}\pm0.36$	$17.8^{a}\pm0.65$	$12.2^{b}\pm0.49$
Mn	$0.76^{c}\pm0.09$	$5.62^{b}\pm0.15$	$7.13^{ab}\pm0.89$	$8.27^{ab}\pm0.98$	$8.78^{a}\pm0.58$
Zn	$1.1^{c}\pm0.08$	$3.73^{b}\pm0.06$	$4.6^{ab}\pm0.45$	$5.28^{a}\pm0.24$	$5.48^{a}\pm0.49$
Cu	$0.33^{b}\pm0.01$	$0.59^{a}\pm0.02$	$0.69^{a}\pm0.01$	$0.72^{a}\pm0.05$	$0.81^{a}\pm0.09$
L*	$28.82^{a}\pm0.16$	$26.54^{b}\pm0.30$	$28.94^{a}\pm0.25$	$27.22^{b}\pm0.25$	$29.23^{a}\pm0.19$
a*	$11.39^{a}\pm0.06$	$7.16^{c}\pm0.10$	$6.22^{d}\pm0.14$	$7.75^{b}\pm0.10$	$6.91^{c}\pm0.22$
b*	$10.54^{a}\pm0.16$	$3.67^{c}\pm0.09$	$3.13^{c}\pm0.18$	$5.29^{b}\pm0.17$	$3.26^{c}\pm0.28$
C*	$15.52^{a}\pm0.11$	$8.04^{c}\pm0.13$	$6.96^{d}\pm0.21$	$9.39^{b}\pm0.18$	$7.65^{cd}\pm0.30$
ΔE	-	$8.41^{a}\pm0.14$	$9.06^{a}\pm0.23$	$6.61^{b}\pm0.18$	$8.58^{a}\pm0.33$

Results are reported as mean ± SEM (n=3). Mean values within the same column followed by different superscript letters (a–c) are significantly different when subjected to Tukey's test ($p < 0.05$). G1: Cookie with 50% replace of butter, G2: Cookie with 50% replace of butter and 10% of wheat flour, G3: Cookie with 75% replace of butter, G4: Cookie with 75% replace of butter and 10% of wheat flour and CH: Carbohydrate, TDF: Total dietary fiber, L*: Lightness, a*: redness, b*: yellowness, C*: chroma, ΔE*: color difference.

Ash content increased progressively with increasing extract incorporation ($p < 0.05$), suggesting mineral enrichment derived from the SMS extract addition. Notably, calcium content in G1 (557.11 mg/100 g) was approximately tenfold higher than in the control (52.45 mg/100 g) ($p < 0.05$). Furthermore, doubling the extract concentration from G1 (31.25 mg/100 g) to G4 (59.4 mg/100 g) resulted in a proportional increase in calcium content ($p < 0.05$). Overall, all analyzed minerals increased significantly with extract addition, showing a concentration-dependent trend ($p < 0.05$). Similar mineral enrichment has been reported in cookies fortified with mushrooms and other agro-industrial by-products [59–62]. Total carbohydrate content decreased in formulations where wheat flour was partially replaced (G2 and G3) compared to the control, G1, and G4 ($p < 0.05$). In contrast, total dietary fiber content increased significantly, from 3.16 g/100 g in the control to 8.33 g/100 g in G4 ($p < 0.05$), consistent with previous studies incorporating *P. ostreatus* into cookies [63]. Based on these results, all formulations could be classified as "high in fiber" according to Regulation (EC) No 1924/2006 [49]. As a consequence of increased fiber content and reduced fat levels, all reformulated cookies exhibited lower energy values than the control. Overall, these results highlight the potential of SMS extract, derived from an agro-industrial by-product, not only as a fat replacer but also as a

 doi:10.20944/preprints202604.1790.v1

functional ingredient capable of improving the nutritional profile of bakery products by enhancing fiber, protein, and mineral contents.

3.3.2. Instrumental Color of Low-Fat Cookies

The surface color of the cookies, expressed as L*, a*, b*, C*, and ΔE values, is presented in Table 9. The incorporation of the SMS extract significantly affected the optical properties of the cookies ($p < 0.05$). Specifically, a* and b* values decreased in all SMS extract–containing formulations compared to the control ($p < 0.05$). The reduction in a* and b* values, resulting in lower chroma (C*), may be attributed to the increased protein content, which provides precursors for Maillard reactions during baking [61]. The ΔE values obtained (6.61–9.06) indicate that the color differences between reformulated and control cookies were perceptible to the human eye, as ΔE values exceeded the threshold of 3 [64]. Among the formulations, G3 exhibited the smallest color difference relative to the control ($p < 0.05$), which may be related to its higher moisture content and lower extract incorporation compared to G4. Similar color changes have been previously reported when fat or wheat flour was replaced with mushroom fruiting bodies or other complex carbohydrates [47,61,62]. Overall, these results indicate that color changes may arise from the inherent color of the added extract used to replace wheat flour and margarine, which differs markedly from the original ingredients [65,66]. As color is a key factor influencing consumer acceptance of food products, a sensory evaluation was conducted to assess the impact of these color changes, as well as potential alterations in other quality attributes resulting from fat and flour replacement. [50].

3.3.3. Sensorial Analysis of Low-Fat Cookies

The sensory evaluation of all cookie formulations, including attributes such as appearance, graininess, hardness, stickiness, sweet taste, bitter taste, and overall acceptability, is presented in Figure 3. Despite the differences observed in instrumental color analysis, no significant differences were perceived by the panelists among any of the formulations compared to the control in terms of color ($p > 0.05$). Similarly, no differences were detected in appearance or graininess ($p > 0.05$). Comparable findings have been reported in studies where wheat flour substitution below 15% was achieved through the incorporation of mushroom powder or *Pleurotus*-derived fiber extracts [58,67]. Likewise, fat replacement using inulin or canned green pea purée did not negatively affect sensory perception in previous studies [59]. In contrast, G4, corresponding to the formulation with 75% fat and 10% wheat flour replacement and the highest extract concentration (23.76%), exhibited significant differences compared to the control in aroma, hardness, stickiness, and bitterness ($p < 0.05$), indicating a stronger influence of extract level and fat and flour reduction on sensory perception [20,21,58]. Similar effects have been reported when mushroom powder exceeded 15% or fiber extracts were incorporated at levels above 12% [58,68]. The SMS extract may contribute aromatic and flavor-active compounds due to the presence of volatile constituents in its composition [3,62]. It is well documented that one of the most critical challenges in fat replacement in bakery products is texture modification, often leading to increased hardness and less desirable mouthfeel [20,21]. In addition, high dietary fiber content has been associated with increased crispiness and hardness [58].

Regarding sweetness, a progressive decrease was observed with increasing extract incorporation, with the lowest hedonic scores recorded for G4 ($p < 0.05$). These results are consistent with previous reports of sweetness reduction following 50% fat substitution [20]. However, no significant differences were found between the control and G1 (50% fat replacement) ($p > 0.05$). Among all formulations, G1 emerged as the most promising prototype, showing no significant differences compared to the control across all evaluated attributes ($p > 0.05$), including overall acceptability, which differed significantly between the control and all other formulations ($p < 0.05$), except for G1. Overall, these results indicate that moderate substitution levels allow sensory properties comparable to the control to be maintained, whereas higher replacement levels may result in noticeable changes in specific sensory attributes. In summary, formulation G1 enabled a substantial

 doi:10.20944/preprints202604.1790.v1

reduction in fat content while simultaneously increasing dietary fiber and protein without compromising the sensory acceptability of cookies [20,22].

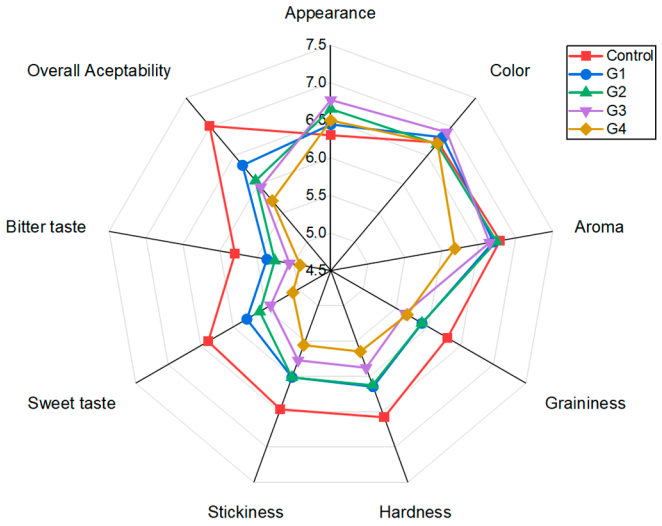

Figure 3. Radial plot of the sensory evaluation results of low-cookies formulated with the different concentrations of SMS extract compared with the control sample.

3.3.4. Kineticstic of Starch Digestion and Glycaemic Index of Low-Fat Cookies

Based on the sensory evaluation results, only formulation G1 was selected for further analysis, as it exhibited the closest sensory profile to the control and the highest overall acceptability. In this context, the nutritional improvement of these cookies was further assessed by evaluating the *in vitro* digestibility of starch. As shown in Figure 4, starch hydrolysis in both the control and G1 began during the oral phase (2 min), driven by the action of salivary α-amylase, with no significant differences observed between samples at this stage ($p > 0.05$). Starch hydrolysis continued during the gastric phase, where, after 20 min, the first significant difference between samples was detected ($p < 0.05$), with hydrolysis values of 45.93% for the control and 27.57% for G1. Subsequently, starch hydrolysis remained relatively unchanged in both samples until the end of the gastric phase at 120 min ($p > 0.05$).

Although the contribution of salivary α-amylase during gastric digestion has traditionally been ignored due to the short contact with the food and the pH shift from 6.9 to approximately 3, residual enzymatic activity during this phase has been reported [69]. Based on *in vitro* digestion kinetics, starch can be classified into rapidly digestible starch (RDS), slowly digestible starch (SDS), and resistant starch (RS) fractions [70]. The RDS fraction corresponds to the starch hydrolyzed within the first 20 min of digestion [71]. Accordingly, replacing 50% of fat with the SMS dietary fiber extract resulted in a significantly lower RDS content compared to the control ($p < 0.05$). Similar reductions in RDS have been previously reported following the incorporation of dietary fiber-rich oyster mushroom or fibers derived from other agro-industrial by-products into cookies [58,72–74]. The reduced starch hydrolysis observed in the reformulated cookies compared to the control may be attributed to the presence of high dietary fiber content in the G1 cookie (6.64 g/100g). Dietary fiber can hinder enzyme–substrate interactions through physical encapsulation of starch granules or by increasing digesta viscosity [61,62,72,74]. In addition, fat content has been reported to play a key role in starch organization within cookie dough, with significant morphological differences observed when fat replacement exceeds 30% [22,23,75].

 doi:10.20944/preprints202604.1790.v1

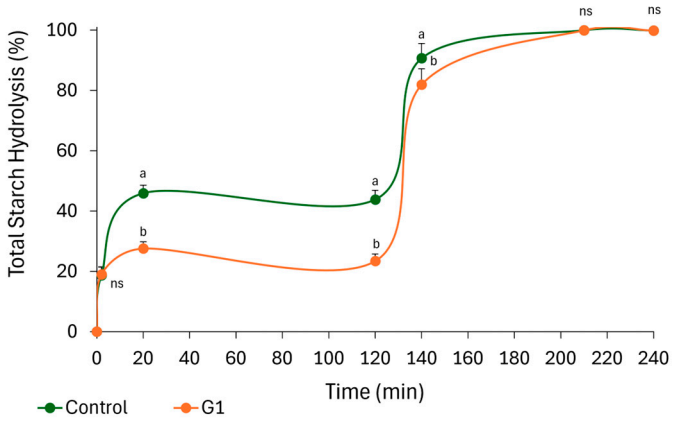

Figure 4. Total starch hydrolysis rate of bread during gastrointestinal digestion. Results are reported as mean±SEM (n=6). Different letters indicated statistical difference when subjected to Tukey's test ($p < 0.05$), ns: non statistically difference. G1: Cookie with 50% replacement of butter.

Upon initiation of the intestinal phase, marked by the addition of pancreatic α-amylase, both samples exhibited a hydrolysis peak at 140 min. In the control, this peak remained stable until the end of the digestion assay at 240 min, with no significant differences observed among 140, 210, and 240 min ($p > 0.05$). In contrast, starch hydrolysis in G1 did not stabilize until 210 min, with no significant differences between 210 and 240 min ($p > 0.05$). As shown in Table 9, although total starch content did not differ between samples ($p > 0.05$), the proportion of starch hydrolyzed at 140 min (SH_{140}) was significantly lower in G1 (81.97%) than in the control (90.70%) ($p < 0.05$). These results further confirm the inhibitory effect of SMS extract incorporation and fat reduction on starch hydrolysis. Consistently, the kinetic constant (k) decreased significantly from 0.03255 in the control to 0.01454 in G1 ($p < 0.05$), indicating slower starch digestion kinetics in the reformulated cookies. The glycemic index (GI) is a nutritional parameter used to classify carbohydrate-rich foods according to their potential to increase postprandial blood glucose levels [76]. Beyond its clinical relevance, GI has been associated with the risk of developing metabolic and cardiovascular diseases [69,71,76]. Since direct measurement of GI in human subjects is time-consuming, invasive, labor-intensive, and costly, *in vitro* methodologies have been developed as a faster and more accessible alternative to predict *in vivo* glycemic (pGI) response [71,76]. In the present study, *in vitro* GI estimation was applied to assess the potential of the SMS extract to modulate the glycemic response of cookies. The area under the curve (AUC) and hydrolysis index (HI) values required for pGI calculation are presented in Table 9.

The physiological impact of dietary fiber incorporation and fat reduction on starch digestion was reflected in a significantly lower AUC_{140} for G1 (6446.24) compared to the control (9940.52) ($p < 0.05$). Accordingly, both HI and pGI values were significantly reduced in G1 relative to the control ($p < 0.05$). Based on GI classification criteria, foods can be categorized as low GI (≤54), medium GI (>55 to <70), or high GI (≥70) [70]. Under this classification, G1 can be considered a medium-GI food, whereas the control formulation falls into the high-GI category. High dietary fiber content is commonly associated with reduced pGI values, and similar reductions have been reported in fiber-enriched cookies compared with conventional formulations [73,74]. Overall, these findings highlight the potential of dietary fiber extracted from SMS to effectively reduce the glycemic impact of cookies while maintaining sensory acceptability comparable to that of conventional products, supporting its application as a functional ingredient in the development of healthier bakery products.

 doi:10.20944/preprints202604.1790.v1

Table 9. Starch digestion parameters of fat low-cookies formulated with a 50% fat reduction and the addition of optimized dietary fiber extract (G1). TS (%): Total Starch (%), SH_{140}: total starch hydrolyzed at 140 min; *k*: kinetic constant; AUC: area under the curve; HI: hydrolysis index; pGI: predicted glycemic index.

Muestras	TS (%)	SH_{140}(%)	k_{140}	AUC_{140}	HI_{140}	pGI_{140}
CT	29.16^{b}±1.32	90.70^{a}±3.06	0.03255^{a} ± 0.0001	9940.52^{a} ± 498.03	84.10^{b}±4.21	85.88^{b}±2.31
G1	33.70^{b}±2.18	81.97^{b}±1.74	0.01454^{b} ±0.0006	6446.24^{b} ± 117.28	54.54^{c}±0.99	69.65^{c}±0.54
Bread	46.54^{a}±0.07	85.69^{ab}±0.94	0.03180^{a} ± 0.0001	9332.73^{a} ±124.14	100.00^{a}±1.33	94.61^{a}±0.73

5. Conclusions

Spent mushroom substrate can be used as a source of dietary fiber, and this fiber can be used to partially replace fat in cookie production. The total dietary fiber content of the extract optimized using the statistical surface response methodology, through the Box-Behnken design, was 30.82%. The chemical and techno-functional characterization of the extract also revealed a high content of proteins and minerals, which provided suitable emulsifying and oil-holding properties. The incorporation of the optimized extract to substitute 50% of fat in cookies (G1) showed significantly higher contents of protein, minerals, and total dietary fiber, reaching levels that allow them to be labeled as "high in fiber" according to European Regulation (EC) No 1924/2006. In addition, G1 exhibited a significant reduction in the predicted glycemic index, which can be attributed to the high dietary fiber content and its ability to form a physical barrier that limits enzymatic access to starch. Importantly, the G1 prototype achieved an overall sensory acceptability comparable to that of the control formulation prepared with a traditional recipe, effectively balancing the health benefits associated with fat reduction and fiber enrichment with the palatability expected in bakery products. Overall, these findings highlight the potential of dietary fiber extract from SMS, using an environmentally friendly technique such as ultrasound-assisted extraction, not only as a strategy for the valorization of an agro-industrial by-product but also as a promising tool for the food industry to develop cookies with an improved nutritional profile. Future research should address the long-term storage stability of these products and the *in vivo* validation of their glycemic response.

Supplementary Materials: The following supporting information can be downloaded at: www.mdpi.com/xxx/s1, Figure S1.

Author Contributions: Conceptualization, P.B-G. and V.G.; methodology, P.B-G., V.G. and P.B.; software, V.G.; validation, P.B-G. and V.G.; formal analysis, P.B-G. and V.G.; investigation, P.B-G., V.G. and P.B.; resources, P.B-G. and V.G.; data curation, P.B-G. and V.G.; writing—original draft preparation, P.B-G. and V.G.; writing—review and editing, P.B-G. and V.G.; visualization, P.B-G. and V.G.; supervision, M.P-C.; project administration, M.P.-C; funding acquisition, M.P-C. All authors have read and agreed to the published version of the manuscript.

Funding: This research was funded by European Regional Development Fund (ERDF), granted to the Autonomous Community of La Rioja within the ERDF Operational Programs 2021–2027 (project number: CT24_05).

Data Availability Statement: The data presented in this study are available on request from the corresponding author.

Conflicts of Interest: The authors declare no conflict of interest.

 doi:10.20944/preprints202604.1790.v1

References

1. A. Kousar, H. A. Khan, S. Farid, Q. Zhao, and I. Zeb. Recent advances on environmentally sustainable valorization of spent mushroom substrate: A review. *Biofuels, Bioprod. Bioref.* **2024**, *18*, 639–651. doi: 10.1002/bbb.2559.
2. J. Guo, M. Zhang, and Z. Fang. Valorization of mushroom by-products: a review. *J. Sci. Food Agric.* **2022**, *102*, 5593–5605, doi: 10.1002/jsfa.11946.
3. H. Moshtaghian, M. Parchami, K. Rousta, and P. R. Lennartsson. Application of Oyster Mushroom Cultivation Residue as an Upcycled Ingredient for Developing Bread. *Applied Sciences* **2022**, *12*, 11067. doi: 10.3390/app122111067.
4. Y. K. Leong, T. W. Ma, J. S. Chang, and F. C. Yang. Recent advances and future directions on the valorization of spent mushroom substrate (SMS): A review. *Elsevier Ltd*. **2022**, *344*, 126157. doi: 10.1016/j.biortech.2021.126157.
5. Antunes, F., Marçal, S., Taofiq, O., Morais, A. M. M. B., Freitas, A. C., Ferreira, I. C. F. R., & Pintado, M. Valorization of mushroom by-products as a source of value-added compounds and potential applications. *Molecules* **2020**, *25*, 2672. doi: 10.3390/molecules25112672.
6. D. Grimm and H. A. B. Wösten. Mushroom cultivation in the circular economy. *Springer Verlag*. **2018**, *102*, 7795–7803. doi: 10.1007/s00253-018-9226-8.
7. S. Catal and A. Peksen. Physical, chemical and biological properties of spent mushroom substrates of different mushroom species. *Acta Hortic.* **2020**, *1287*, 353–360. doi: 10.17660/ActaHortic.2020.1287.45.
8. S. S. Lam *et al.* Microwave vacuum pyrolysis conversion of waste mushroom substrate into biochar for use as growth medium in mushroom cultivation. *J. Chem. Technol. Biotechnol.* **2019**, *94*, 1406–1415. doi: 10.1002/jctb.5897.
9. K. Guo, Yaping; Zhang, Guoqing; Chen, Qingjun; Yang. Analysis on Bacterial Community Structure in Mushroom (*Agaricus bisporus*) Compost Using PCR-DGGE. *Agricultural Science & Technology* **2015**, *16*, 1778–1784.
10. Y. Tian *et al.* Ultrasonic-assisted extraction and antioxidant activity of polysaccharides recovered from white button mushroom (*Agaricus bisporus*). *Carbohydr. Polym.* **2012**, *88*, 522–529. doi: 10.1016/j.carbpol.2011.12.042.
11. I. Aguiló-Aguayo, J. Walton, I. Viñas, and B. K. Tiwari. Ultrasound assisted extraction of polysaccharides from mushroom by-products. *LWT*, **2017**, *77*, 92–99. doi: 10.1016/j.lwt.2016.11.043.
12. P. Ayuso, J. Quizhpe, R. Peñalver, P. García-Pérez, and G. Nieto. Green Valorization Strategies of *Pleurotus ostreatus* and Its By-Products: A Critical Review of Emerging Technologies and Sustainable Applications. *Molecules* **2025**, *30*, 4318. doi: 10.3390/molecules30214318.
13. A. Sulaiman and F. V. M. Silva. Principles of sonication and its equipment in the food industry. In *Non-thermal Food Processing Operations: Unit Operations and Processing Equipment in the Food Industry*, Elsevier Inc., Netherlands, Amsterdam, 2023, 435–464. doi: 10.1016/B978-0-12-818717-3.00001-9.
14. M. Sun, Y. Zhuang, Y. Gu, G. Zhang, X. Fan, and Y. Ding. A comprehensive review of the application of ultrasonication in the production and processing of edible mushrooms: Drying, extraction of bioactive compounds, and post-harvest preservation. *Ultrasonics Sonochemistry* **2024**, *102*, 106763 doi: 10.1016/j.ultsonch.2024.106763.
15. F. Chemat, N. Rombaut, A. G. Sicaire, A. Meullemiestre, A. S. Fabiano-Tixier, and M. Abert-Vian. Ultrasound assisted extraction of food and natural products. Mechanisms, techniques, combinations, protocols and applications. A review. *Ultrason. Sonochem.* **2017**, *34*, 540–560. doi: 10.1016/J.ULTSONCH.2016.06.035.
16. K. Wang *et al.* Ultrasound-assisted extraction of polysaccharide from spent *Lentinus edodes* substrate: Process optimization, precipitation, structural characterization and antioxidant activity. *Int. J. Biol. Macromol.* **2021**, *191*, 1038–1045. doi: 10.1016/j.ijbiomac.2021.09.174.
17. S. J. Klausen, A. B. Falck-Ytter, K. O. Strætkvern, and C. Martin. Evaluation of the Extraction of Bioactive Compounds and the Saccharification of Cellulose as a Route for the Valorization of Spent Mushroom Substrate. *Molecules* **2023**, *28*, 13. doi: 10.3390/molecules28135140.

 doi:10.20944/preprints202604.1790.v1

18. Y. Bai, F. Liang, Y. Yang, L. Guan, and H. Ma. Polysaccharides from edible fungi spent mushroom substrates: A review of their extraction, purification, structural characteristics, and biological activities. *Int. J. Biol. Macromol.* **2025**, *330*, 147925. doi: 10.1016/j.ijbiomac.2025.147925.
19. A. Devi and B. S. Khatkar. Physicochemical, rheological and functional properties of fats and oils in relation to cookie quality: a review. *J Food Sci Technol.* **2016**, *53*, 3633–3641. doi: 10.1007/s13197-016-2355-0.
20. M. Krystyjan, D. Gumul, R. Ziobro, and M. Sikora. The Effect of Inulin as a Fat Replacement on Dough and Biscuit Properties. *J. Food Qual.* **2015**, *38*, 305–315. doi: 10.1111/jfq.12148.
21. A. Forker, S. Zahn, and H. Rohm. A Combination of Fat Replacers Enables the Production of Fat-reduced Shortdough Biscuits with High-sensory quality. *Food Bioproc. Tech.* **2012**, *5*, 2497–2505. doi: 10.1007/s11947-011-0536-4.
22. L. Laguna, C. Primo-Martín, P. Varela, A. Salvador, and T. Sanz. HPMC and inulin as fat replacers in biscuits: Sensory and instrumental evaluation. *LWT*, **2014**, *56*, 494–501. doi: 10.1016/j.lwt.2013.12.025.
23. J. Rodríguez-García, L. Laguna, A. Puig, A. Salvador, and I. Hernando. Effect of Fat Replacement by Inulin on Textural and Structural Properties of Short Dough Biscuits. *Food Bioproc. Tech.* **2013**, *6*, 2739–2750. doi: 10.1007/s11947-012-0919-1.
24. J. C. Mathers. Dietary fibre and health: the story so far. *Cambridge University Press*. **2023**, *82*, 120–129. doi: 10.1017/S0029665123002215.
25. L. Lin *et al.* Antioxidative and renoprotective effects of residue polysaccharides from *Flammulina velutipes*. *Carbohydr. Polym.* **2016**, *146*, 388–395. doi: 10.1016/j.carbpol.2016.03.071.
26. H. Zhu, K. Sheng, E. Yan, J. Qiao, and F. Lv. Extraction, purification and antibacterial activities of a polysaccharide from spent mushroom substrate. *Int. J. Biol. Macromol.* **2012**, *50*, 840–843. doi: 10.1016/j.ijbiomac.2011.11.016.
27. J. Zhang, G. Meng, G. Zhai, Y. Yang, H. Zhao, and L. Jia. Extraction, characterization and antioxidant activity of polysaccharides of spent mushroom compost of *Ganoderma lucidum*. *Int. J. Biol. Macromol.* **2016**, *82*, 432–439. doi: 10.1016/j.ijbiomac.2015.10.016.
28. Y. Wang *et al.* Extraction, purification and physicochemical properties of a novel lectin from *Laetiporus sulphureus* mushroom. *LWT* **2018**, *91*, 151–159. doi: 10.1016/j.lwt.2018.01.032.
29. AOAC, AOAC Official Method 991.43 Total, Soluble and Insoluble Dietary Fibre in Foods. In *AOAC Official Method of Analysis,* Association of Official Analytical Chemists: Gaithersburg, MD, USA, volume 32. 1995.
30. AOAC, Official Methods of Analysis of AOAC International. Association of Official Analytical Chemists, 17th ed. Gaithersburg, MD, USA, 2000.
31. L. F. Eggers and D. Schwudke. Liquid Extraction: Folch. *Encyclopedia of Lipidomics*. Springer: Netherlands, 2016, 1–6. doi: 10.1007/978-94-007-7864-1_89-1.
32. C. F. Chau and Y. L. Huang. Comparison of the chemical composition and physicochemical properties of different fibers prepared from the peel of *citrus sinensis* L. Cv. Liucheng. *J. Agric. Food Chem.* **2003**, *51*, 2615–2618. doi: 10.1021/jf025919b.
33. L. R. Beuchat. Functional and Electrophoretic Characteristics of Succinylated Peanut Flour Protein. *J. Agric. Food Chem.* **1977**, *25*, 258–261. doi: https://doi.org/10.1021/jf60210a044.
34. K. Yasumatsu *et al.* Whipping and Emulsifying Properties of Soybean Products. *Agric. Biol. Chem.* **1972**, *36*, 719–727. doi: 10.1080/00021369.1972.10860321.
35. C. W. Coffmann and V. V Garcia. Functional properties and amino acid content of a protein isolate from mung bean flour *. *J. Fd Technol* **1977**, *12*, 473–484.
36. A. Brodkorb *et al.* INFOGEST static *in vitro* simulation of gastrointestinal food digestion. *Nat. Protoc,* 2019, 14, 991–1014. doi: 10.1038/s41596-018-0119-1.
37. I. Goñi, A. Garcia-AIonso, and F. Saura-Calixto. A starch hydrolysis procedure to estimate glycemic index. *Nutrition Research* **1997**, *17*, 427–437.
38. F. Chemat, N. Rombaut, A. G. Sicaire, A. Meullemiestre, A. S. Fabiano-Tixier, and M. Abert-Vian. Ultrasound assisted extraction of food and natural products. Mechanisms, techniques, combinations, protocols and applications. A review. *Ultrasonics Sonochemistry* **2017**, *34*, 540–560. doi: 10.1016/j.ultsonch.2016.06.035.

 doi:10.20944/preprints202604.1790.v1

39. H. XuJie and C. Wei. Optimization of extraction process of crude polysaccharides from wild edible *BaChu* mushroom by response surface methodology. *Carbohydr. Polym.* **2008**, *72*, 67–74. doi: 10.1016/j.carbpol.2007.07.034.
40. L. Galvan D'Alessandro, K. Kriaa, I. Nikov, and K. Dimitrov. Ultrasound assisted extraction of polyphenols from black chokeberry. *Sep. Purif. Technol.* **2012**, *93*, 42–47. doi: 10.1016/j.seppur.2012.03.024.
41. T. Z. S. T. X. W. Z. L. and J. L. Ziyi Yang. Optimization of the Extraction Process and Physico- chemical Properties of Soluble Dietary Fiber from Defatted Rice Bran. *Bioresources* **2025**, *20*, 11098–11113. doi:10.15376/biores.20.4.11098-11113.
42. X. Yu, K. Zhu, F. Hu, R. Hu, and W. Dong. Effects of ultrasonic treatment on the physicochemical, structural, and functional properties of soluble dietary fiber from coffee peels. *Ultrason. Sonochem.* **2025**, *114*, 107247. doi: 10.1016/j.ultsonch.2025.107247.
43. W. Vilcapoma *et al.* Optimization of Ultrasound-Assisted Extraction of Dietary Fiber from Yellow Dragon Fruit Peels and Its Application in Low-Fat Alpaca-Based Sausages. *Foods* **2023**, *12*, 2945. doi: 10.3390/foods12152945.
44. H. Yoshikawa, A. Hirano, T. Arakawa, and K. Shiraki. Mechanistic insights into protein precipitation by alcohol. *Int. J. Biol. Macromol.* 2012, 50, 865–871. doi: 10.1016/j.ijbiomac.2011.11.005.
45. P. He, F. Li, L. Huang, D. Xue, W. Liu, and C. Xu. Chemical characterization and antioxidant activity of polysaccharide extract from spent mushroom substrate of *Pleurotus eryngii*. *J. Taiwan Inst. Chem. Eng.* **2016**, *69*, 48–53. doi: 10.1016/j.jtice.2016.10.017.
46. Y. Zhong *et al.* Recent advances in the structure and immunomodulatory activity of food-derived glycoprotein complex. *Journal of Future Foods* **2025**, *5*, 542–550. doi: 10.1016/j.jfutfo.2024.11.002.
47. T. Zhang *et al.* Plant-based fat substitutes with promising functional properties and health benefits. *J Am Oil Chem Soc.* **2024**, *101*, 1183–1196. doi: 10.1002/aocs.12797.
48. H. Pastell, T. Putkonen, and H. Rita. Dietary fibre in legumes, seeds, vegetables, fruits and mushrooms: Comparing traditional and semi-automated filtration techniques. *Journal of Food Composition and Analysis* **2019**, *75*, 1–7. doi: 10.1016/j.jfca.2018.09.011.
49. European Commission, "Regulation (EC) No 1924/2006 with regard to the list of nutrition claims," *Official Journal of the European Union*, Nov. 2012.
50. A. Ambujakshan and R. Baskaran. Insoluble and soluble dietary fiber from banana (*Musa* spp. Grand naine) flower and bract as potential functional ingredients: *In vitro* studies on functional, adsorption and antioxidant properties. *Food Chem.* **2025**, *495*, 146334. doi: 10.1016/j.foodchem.2025.146334.
51. Y. Liu *et al.* Effects of ultrasonic treatment and homogenization on physicochemical properties of okara dietary fibers for 3D printing cookies. *Ultrason. Sonochem.* **2021**, *77*, 105693. doi: 10.1016/j.ultsonch.2021.105693.
52. Z. Ni *et al.* Physicochemical properties, antioxidant activities and hypoglycemic effects of soluble dietary fibers purified from *Lentinula edodes*. *Food Science and Technology* **2023**, *43*, e131122. doi: 10.1590/fst.131122.
53. R. Lucas-González, M. Viuda-Martos, J. Á. Pérez-Álvarez, and J. Fernández-López. Evaluation of Particle Size Influence on Proximate Composition, Physicochemical, Techno-Functional and Physio-Functional Properties of Flours Obtained from Persimmon (*Diospyros kaki* Trumb.) Coproducts. *Plant Foods for Human Nutrition* **2017**, *72*, 67–73. doi: 10.1007/s11130-016-0592-z.
54. E. J. Kim and K. Y. Yoon. Effects of different extraction methods on the physicochemical properties and biological activities of polysaccharides from maca roots. *CYTA - Journal of Food* **2023**, *21*, 596–605. doi: 10.1080/19476337.2023.2252879.
55. W. Dong, D. Wang, R. Hu, Y. Long, and L. Lv. Chemical composition, structural and functional properties of soluble dietary fiber obtained from coffee peel using different extraction methods. *Food Research International* **2020**, *136*, 109497. doi: 10.1016/j.foodres.2020.109497.
56. S. De, P. Chawla, S. B. Dhull, G. Goksen, A. D. Arjun, and A. Bains. Techno-Functional Biochemical Analysis and Food Applications of Edible Mushroom Powder. *Journal of Food Biochemistry* **2025**, *2025*, 21. doi: 10.1155/jfbc/2888689.

 doi:10.20944/preprints202604.1790.v1

57. D. Aggarwal, L. Sabikhi, and M. H. Sathish Kumar. Formulation of reduced-calorie biscuits using artificial sweeteners and fat replacer with dairy-multigrain approach. *NFS Journal* **2016**, *2*, 1–7. doi: 10.1016/j.nfs.2015.10.001.
58. S. H. Ng, S. D. Robert, W. A. N. Wan Ahmad, and W. R. Wan Ishak. Incorporation of dietary fibre-rich oyster mushroom (*Pleurotus sajor-caju*) powder improves postprandial glycaemic response by interfering with starch granule structure and starch digestibility of biscuit. *Food Chem.* **2017**, *227*, 358–368. doi: 10.1016/j.foodchem.2017.01.108.
59. M. Goubgou, L. T. Songré-Ouattara, F. Bationo, H. Lingani-Sawadogo, Y. Traoré, and A. Savadogo. Biscuits: a systematic review and meta-analysis of improving the nutritional quality and health benefits. *Food Production, Processing and Nutrition* **2021**, *3*, 26. doi: 10.1186/s43014-021-00071-z.
60. F. Salehi. Characterization of different mushrooms powder and its application in bakery products: A review. *Int. J. Food Prop.* **2019**, *22*, 1375–1385. doi: 10.1080/10942912.2019.1650765.
61. A. A. Sulieman *et al.* Rheological and quality characteristics of composite gluten-free dough and biscuits supplemented with fermented and unfermented Agaricus bisporus polysaccharide flour. *Food Chem.* **2019**, *271*, 193–203. doi: 10.1016/j.foodchem.2018.07.189.
62. A. Sławińska, E. Jabłońska-Ryś, and W. Gustaw. Physico-Chemical, Sensory, and Nutritional Properties of Shortbread Cookies Enriched with Agaricus bisporus and *Pleurotus ostreatus* Powders. *Appl. Sci.* **2024**, *14*, 1938. doi: 10.3390/app14051938.
63. A. Sławińska, B. G. Sołowiej, W. Radzki, and E. Fornal. Wheat Bread Supplemented with Agaricus bisporus Powder: Effect on Bioactive Substances Content and Technological Quality. *Foods* **2022**, *11*, 3786–3804. doi: 10.3390/foods11233786.
64. S. Onacik-Gür, A. Zbikowska, and A. Jaroszewska. Effect of high-oleic sunflower oil and other pro-health ingredients on physical and sensory properties of biscuits. *CYTA - Journal of Food* **2015**, *13*, 621–628. doi: 10.1080/19476337.2015.1032358.
65. A. Hidalgo, L. Fongaro, and A. Brandolini. Colour screening of whole meal flours and discrimination of seven Triticum subspecies. *J. Cereal Sci.* **2017**, *77*, 9–16. doi: 10.1016/j.jcs.2017.07.006.
66. S. Pădure. The Quantification of Fatty Acids, Color, and Textural Properties of Locally Produced Bakery Margarine. *Appl. Sci.* **2022**, *12*, 1731. doi: 10.3390/app12031731.
67. M. I. Ibrahium and A. I. Hegazy. Effect of Replacement of Wheat Flour with Mushroom Powder and Sweet Potato Flour on Nutritional Composition and Sensory Characteristics of Biscuits. *Curr. Sci. Int.* **2014**, *3*, 26–33.
68. Y. Biao, X. Chen, S. Wang, G. Chen, D. J. Mcclements, and L. Zhao. Impact of mushroom (*Pleurotus eryngii*) flour upon quality attributes of wheat dough and functional cookies-baked products. *Food Sci. Nutr.* **2020**, *8*, 361–370. doi: 10.1002/fsn3.1315.
69. R. Lucas-González, J. Ángel Pérez-Álvarez, S. Moscaritolo, J. Fernández-López, G. Sacchetti, and M. Viuda-Martos. Evaluation of polyphenol bioaccessibility and kinetic of starch digestion of spaghetti with persimmon (*Dyospyros kaki*) flours coproducts during *in vitro* gastrointestinal digestion. *Food Chem.* 2021, 338, 128142–128152. doi: 10.1016/j.foodchem.2020.128142.
70. K. M. Kamil, A. J. Rohana, W. M. I. W. Mohamed, and W. R. W. Ishak. Effect of incorporating dietary fiber sources in bakery products on glycemic index and starch digestibility response: a review. *Nutrire* **2023**, *48*, 36. doi: 10.1186/s41110-023-00220-z.
71. D. Freitas *et al.* Starch digestion: A comprehensive update on the underlying modulation mechanisms and its *in vitro* assessment methodologies. *Trends in Food Science & Technology* **2025**, *159*, 104969. doi: 10.1016/j.tifs.2025.104969.
72. X. Ning *et al.* Cookies fortified with purple passion fruit epicarp flour: Impact on physical properties, nutrition, *in vitro* starch digestibility, and antioxidant activity. *Cereal Chem.* **2021**, *98*, 328–336. doi: 10.1002/cche.10367.
73. E. Agama-Acevedo, J. J. Islas-Hernández, G. Pacheco-Vargas, P. Osorio-Díaz, and L. A. Bello-Pérez. Starch digestibility and glycemic index of cookies partially substituted with unripe banana flour. *LWT* **2012**, *46*, 177–182. doi: 10.1016/j.lwt.2011.10.010.

 doi:10.20944/preprints202604.1790.v1

74. P. Naknaen, T. Itthisoponkul, A. Sondee, and N. Angsombat. Utilization of watermelon rind waste as a potential source of dietary fiber to improve health promoting properties and reduce glycemic index for cookie making. *Food Sci. Biotechnol.* **2016**, *25*, 415–424. doi: 10.1007/s10068-016-0057-z.
75. H. Erinc, B. Mert, and A. Tekin. Different sized wheat bran fibers as fat mimetic in biscuits: its effects on dough rheology and biscuit quality. *J. Food Sci. Technol.* **2018**, *55*, 3960–3970. doi: 10.1007/s13197-018-3321-9.
76. L. S. Sciarini, M. C. Bustos, M. B. Vignola, C. Paesani, C. N. Salinas, and G. T. Pérez. A study on fibre addition to gluten free bread: its effects on bread quality and *in vitro* digestibility. *J. Food Sci. Technol.* **2017**, *54*, 244–252. doi: 10.1007/s13197-016-2456-9.